Lens model for Frontier Fields cluster Abell 2744
Version 1: August 30, 2013

Traci Johnson & Keren Sharon

tljohn@umich.edu, kerens@umich.edu

University of Michigan, Department of Astronomy, 500 Church Street, Ann Arbor, MI 48109, USA

Overview

We present our strong lens model of the Frontier Fields cluster Abell 2744 and files necessary for the creation of magnification maps and errors covering the entire HST ACS field of view ($202'' \times 202''$). We document the methods used in creating the model, the model inputs, and the best-fit model parameters. The deliverables include high-resolution magnification maps for $z = 1, 2, 4,$ and 9, two-dimensional deflection angles, convergence, and shear maps, along with lower-resolution convergence and shear maps from a simulation of 100 models selected periodically from the MCMC chain which can be used to derive magnification maps and errors for any source plane redshift.

We assume a flat ΛCDM cosmology, with $\Omega_\Lambda = 0.7$, $\Omega_M = 0.3$, and $H_0 = 70$ km s^{-1}, where $1'' = 4.54$ kpc at the cluster redshift $z = 0.308$.

Lens Model

Our lens modeling method is parametric in nature. We use the publicly-available software `LENSTOOL` (Jullo et al. 2007), which utilizes a Markov Chain Monte Carlo to find the best-fit parameters for each mass component and arc redshift weighted by Bayesian evidence. We search the parameter space for the best-fit solution in an iterative process. We start by placing masses typical of most clusters near the center of the light distribution, and then build up the model in complexity with each iteration by adding more image constraints and more mass components. Each iteration is completed under source plane optimization, where the rms scatter used to rank models is computed when the images are traced back to the source plane. We plan to revise this model using image plane optimization in future versions. The latter method is more computationally intensive and more effective at reducing scatter in the image plane; however, the source plane optimization we are presenting produces a

reasonably low rms scatter. We have visually inspected the model and verified that it does not predict counter images that are not detected in the data above the detection threshold.

We use the arcs identified by Merten et al. (2011) as constraints for the lens model, along with those made by Johan Richard (private communication). In total, we have 60 images from 17 unique background sources. We fix the redshifts of arcs # 4 and 6 to the spectroscopic redshifts obtained by Richard et al. (in prep.). For the rest of the arcs, we use the ranges of photometric redshifts from Merten et al. (2011) and those computed from preliminary HST imaging (Dan Coe, private communication) as initial Bayesian priors; however, we allow for the optimization to extend beyond this range if needed in order to solve for the best-fit redshift. A list of the arcs and their redshifts (spectroscopic, photometric, and model-derived with priors) is given in Table 1.

Our lens model includes four cluster-scale halos and halos assigned to each individual red sequence cluster member galaxy, all represented by pseudo-isothermal elliptical mass distributions (PIEMD; Limousin et al. 2005). The PIEMD is parameterized by a two-dimensional location in the lens plane, a lens plane redshift, ellipticity and position angle, a fiducial velocity dispersion, and core radius and cut radius. The galaxies used in the model are selected by color; those falling on the red sequence at the cluster redshift are considered cluster members. The PIEMD halo for each galaxy is scaled by light in the ACS F814W band according to the relationships in Limousin et al. (2005),

$$\begin{aligned} \sigma_0 &= \sigma_0^\star \left(\frac{L}{L^\star}\right)^{1/2} \\ r_{\rm core} &= r_{\rm core}^\star \left(\frac{L}{L^\star}\right)^{1/4} \\ r_{\rm cut} &= r_{\rm cut}^\star \left(\frac{L}{L^\star}\right)^{1/4} . \end{aligned}$$

We find that an $L^\star$ galaxy at $z = 0.308$ has an ACS F814W magnitude of 18.50 and set $\sigma_0^\star = 120$ km s^{-1}, $r_{\rm core}^\star = 0.15$ kpc, and $r_{\rm cut}^\star = 30$ kpc, following Limousin et al. (2008). These parameters are not well constrained by the lens model, since these halos have small, localized effects on the lensing potential. We allow only two cluster member galaxies (including the brightest cluster galaxy) to be optimized using their light-scaled PIEMD parameter values as priors. Our best-fit model includes 82 constraints and 45 free parameters, and produces an image plane rms scatter of $0.53''$. The model details are included in Table 2.

Deliverables

We have computed magnification maps for source redshift planes of $z = 1, 2, 4,$ and 9. We also include the x and y deflection maps, representing the deflection angle from image plane to source plane in units of arcseconds, and the convergence κ and shear γ maps, all computed at a redshift of $z = 9$. These additional maps can be used to calculate the magnifications at any source plane redshift. We also include a lower resolution convergence and shear maps for 100 models selected at equal intervals throughout the MCMC chain, which can be used to derive the magnification errors at any source redshift. A summary of the model files is given in Table 3.

Each high-resolution map is a square $202.08'' \times 202.08''$ grid oriented north up and east to the left, with a pixel scale of $0.03''$. The lower-resolution maps are set to a pixel scale of $0.12''$. The FITS WCS astrometry has been matched to the preliminary HST science products created by Anton Koekemoer.[1]

Modeling strengths and caveats

Our model best describes the magnifications in the strong lensing regime, or the region more or less enclosed by the strongly-lensed arcs (for Abell 2744 the largest image separation is $\sim 80''$ around cluster center). Therefore, the objects within a few arcseconds of any images used as constraints in our model will have the most precise magnifications, especially if those images had fixed spectroscopic redshifts. The regions of the map that are most vulnerable to both systematic and modeling error are near the critical curve and far from any image constraints.

We do not recommend the use of our model for computing the magnifications in the "blank" parallel field. Extrapolating our model out to this field predicts $\mu < 1.2$ (see Figure 1), which is expected if the field is truly blank, or unmagnified ($\mu = 1$). We do not account for any mass outside of the combined FOV of existing HST data (additional cluster members, large-scale structure, etc.) which could boost the lensing in this region, thus, this extrapolation results in a crude, unconstrained estimate of the magnification. For the parallel field, we suggest that one uses maps generated by other mapping techniques, which include weak lensing as constraints.

---

[1] e.g. http://archive.stsci.edu/pub/hlsp/frontier/internal/abell2744/images/hst/hlsp_frontier_hst_acs-30mas_abell2744_f606w_v0.2_drz.fits.

Future model revisions

The magnification maps we have created in this model version of Abell 2744 are at this moment very well constrained and provide precise values for the magnification in the strong lensing regime. However, no model is exact and can alway be improved upon. New arc identifications can add constraint to new regions of the map and spectroscopic redshifts of arcs can greatly reduce magnification errors in areas near those images. We will use our current models to identify new image systems and include them in new model version and will update known image systems with new spectroscopic redshifts as they become available. Updated versions will be computed under image plane optimization.

REFERENCES

Jullo, E., Kneib, J.-P., Limousin, M., et al. 2007, New Journal of Physics, 9, 447

Limousin, M., Kneib, J.-P., & Natarajan, P. 2005, MNRAS, 356, 309

Limousin, M., Richard, J., Kneib, J.-P., et al. 2008, A&A, 489, 23

Merten, J., Coe, D., Dupke, R., et al. 2011, MNRAS, 417, 333

This preprint was prepared with the AAS LaTeX macros v5.2.

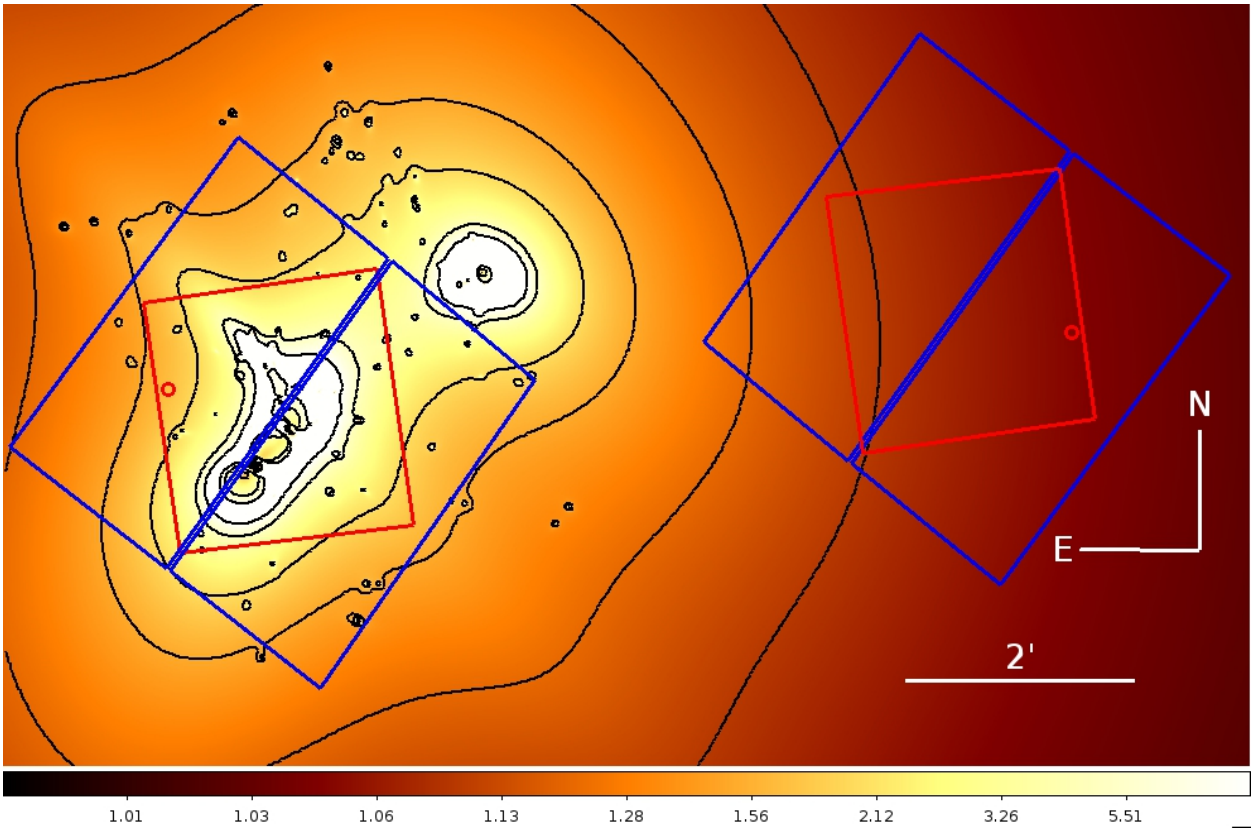

Fig. 1.— Magnification maps centered on the HST Frontier Field cluster Abell 2744 (left) and parallel field for a source redshift of $z = 9$. Overlaid are the CCD chip boundaries of the ACS (blue) and WFC3/IR (red) for both Frontier Field pointings. Magnification contour levels are $\mu = 1.1, 1.2, 1.5, 2, 5, 10$.

Table 1. Modeling constraints

Image system	R.A.	Dec.	Spec z[a]	Photo z[b]	Photo z[c]	Model z[d]	z priors[e]	Image plane rms ($''$)	Ref.
1a.1	00:14:23.41	-30:24:14.10	···	2.0 ± 0.3	···	$1.64^{+0.07}_{-0.04}$	1.4-2	0.19	1
1a.2	00:14:23.03	-30:24:24.56							
1a.3	00:14:20.69	-30:24:35.95							
1b.1	00:14:23.29	-30:24:17.11						0.15	
1b.2	00:14:23.14	-30:24:22.05							
1b.3	00:14:20.58	-30:24:36.44							
2a.1	00:14:19.98	-30:24:12.06	···	2.0 ± 0.3	···	$2.01^{+0.11}_{-0.03}$	1.5-2.4	0.32	1
2a.2	00:14:23.35	-30:23:48.21							
2a.3[f]	00:14:20.50	-30:23:59.63							
2a.4	00:14:20.74	-30:24:07.66							
2b.1	00:14:19.81	-30:24:08.18						0.44	
2b.2	00:14:23.22	-30:23:46.68							
2b.3	00:14:20.28	-30:23:57.43							
2b.4[f]	00:14:20.70	-30:24:03.06							
3.1	00:14:21.45	-30:23:37.95	···	4.0 ± 0.3	···	$2.92^{+0.14}_{-0.33}$	2.0-3.5	0.74	1
3.2[f]	00:14:21.31	-30:23:37.69							
3.3	00:14:18.60	-30:23:58.44							
4.1	00:14:22.11	-30:24:09.48	3.58	···	···	···	···	0.64	1
4.2	00:14:22.95	-30:24:05.84							1
4.3	00:14:19.30	-30:24:32.13							1
4.4	00:14:22.37	-30:24:17.69							2
4.5	00:14:22.46	-30:24:18.38							2
5.1	00:14:20.02	-30:23:31.45	···	4.0 ± 0.5	···	4.28	1.8-5.0	0.27	1
5.2	00:14:20.40	-30:23:28.95							
5.3	00:14:19.19	-30:23:41.14							
6.1	00:14:23.65	-30:24:06.48	2.019	···	···	···	···	0.14	1
6.2	00:14:22.57	-30:24:28.84							
6.3	00:14:20.74	-30:24:33.74							
7.1	00:14:23.58	-30:24:08.35	···	3.7 ± 0.5	2.7-3.3	$2.65^{+0.16}_{-0.10}$	2.3-3.3	0.16	1
7.2	00:14:22.85	-30:24:26.73							
7.3	00:14:20.30	-30:24:35.33							
8.1	00:14:21.53	-30:23:39.62	···	4.0 ± 0.2	···	$1.72^{+0.16}_{-0.47}$	1.0-2.8	0.43	1
8.2	00:14:21.32	-30:23:39.20							
9.1	00:14:21.21	-30:24:18.98	···	3.0 ± 0.5	1.0-2.5	$4.35^{+0.58}_{-0.23}$	3.3-6.5	1.05	1
9.2	00:14:20.91	-30:24:22.47							
9.3	00:14:24.04	-30:23:49.75							
10.1	00:14:21.22	-30:24:21.16	···	3.0 ± 0.5	2.5-3.1	$6.4^{+1.2}_{-0.6}$	4.0-9.0	0.52	1
10.2	00:14:20.97	-30:24:23.33							
10.3	00:14:24.17	-30:23:49.56							
11.1	00:14:21.93	-30:24:13.89	···	3.0 ± 0.5	1.4-3.2	$2.69^{+0.12}_{-0.15}$	2.0-3.3	0.44	1
11.2	00:14:23.34	-30:24:05.23							1
11.3	00:14:19.87	-30:24:32.09							1
11.4	00:14:22.69	-30:24:23.55							2
12.1	00:14:22.47	-30:24:16.09	···	···	1.5-3.1	5.125	4.0-6.8	0.36	2

Table 1—Continued

Image system	R.A.	Dec.	Spec z[a]	Photo z[b]	Photo z[c]	Model z[d]	z priors[e]	Image plane rms ($''$)	Ref.
12.2	00:14:22.38	-30:24:11.72							
12.3	00:14:22.70	-30:24:10.76							
12.4	00:14:19.07	-30:24:35.83							
13.1	00:14:22.17	-30:24:09.21	···	···	0.6-2.5	$1.38^{+0.05}_{-0.03}$	1.2-1.8	0.15	2
13.2	00:14:22.51	-30:24:07.79							
13.3	00:14:19.87	-30:24:28.96							
14.1	00:14:21.54	-30:23:40.69	···	···	1.8-3.2	$1.72^{+0.18}_{-0.38}$	1.0-2.3	0.49	2
14.2	00:14:21.23	-30:23:39.97							
16.1	00:14:13.57	-30:22:32.91	···	···	2.6-3.7	1.27	0.5-8.0	0.66	2
16.2	00:14:13.53	-30:22:36.36							
16.3	00:14:13.10	-30:22:45.51							
17.1	00:14:13.77	-30:22:41.53	···	···	···	$0.73^{+1.12}_{-0.03}$	0.4-7.0	1.04	2
17.2	00:14:13.79	-30:22:40.94							
17.3	00:14:13.82	-30:22:39.49							
18.1	00:14:21.78	-30:23:44.02	···	···	1.5-5.3	1.72	1.5-2.5	0.38	3
18.2	00:14:21.21	-30:23:44.29							

[a]Spectroscopic redshift measured by J. Richard (in prep).

[b]Photometric redshifts listed by Merten et al. (2011).

[c]Range of photometric redshifts (95% confidence level) from preliminary HST imaging (Dan Coe, private communication).

[d]Errors in model redshift represent the 1σ distribution in redshifts from the MCMC chain and are only reported when the distribution is close to Gaussian.

[e]Bayesian priors are for the final model iteration.

[f]Coordinates revised by J. Richard (private communication).

References. — (1) Merten et al. (2011), (2) J. Richard (private communication), (3) A. Zitrin (private communication).

Table 2. Details of Len Model

Component	ΔRA (″)	ΔDec (″)	e	θ (°)	$r_{\rm core}$ (kpc)	$r_{\rm cut}$ (kpc)	σ (km s^{-1})
cluster halo #1	19.1 ± 0.4	$-17.9^{+0.3}_{-0.11}$	$0.49^{+0.06}_{-0.03}$	$32.7^{+3.7}_{-6.8}$	$9.95^{+1.3}_{-2.0}$	[1500]	476^{+15}_{-30}
cluster halo #2	13.8 ± 9	37.3 ± 5	0.892 (0.5-0.95)	$-48.1^{+8.0}_{-1.1}$	$57.1^{+9.3}_{-25}$	[1500]	569^{+37}_{-72}
cluster halo #3	$8.2^{+2.3}_{-0.2}$	$-5.2^{+2.9}_{-0.3}$	$0.63^{+0.08}_{-0.02}$	65.2 (56-68)	$92.1^{+9.6}_{-11}$	[1500]	861^{+76}_{-4}
cluster halo #4	$-101.8^{+5.5}_{-0.8}$	$84.7^{+1.4}_{-0.8}$	$0.274^{+0.12}_{-0.10}$	-44.0^{+16}_{-6}	$41.2^{+17.7}_{-28}$	[1500]	799 (400-900)
BCG	[0.000]	[0.000]	$0.37^{+0.24}_{-0.15}$	85.7^{+18}_{-9}	2.90 (0-7)	263 (0-800)	305 (230-480)
galaxy	[-90.4]	[80.3]	[0.260]	[36.2]	[0.539]	[74.9]	131 (0-200)
$L^\star$ galaxy	···	···	···	···	[0.15]	[30]	[120]

Note. — Parameters for best-fit model and Gaussian 1σ errors derived from the parameter values in the MCMC chain. We report the Bayesian priors for the final model iteration in parentheses when a Gaussian does not fit the distribution of parameter values. Values in brackets are not optimized, or "frozen" parameters. ΔRA and ΔDec are measured with respect to the galaxy at α=00:14:20.702, δ=-30:24:00.62, position angles are measured north of west.

Table 3. List of Delivered Files

File name	Deliverable	Source redshift	Size [pixels]	Pixel scale [″]
...mag-z1...	magnification map (μ)	1	6736×6736	0.03
...mag-z2...	magnification map (μ)	2	6736×6736	0.03
...mag-z4...	magnification map (μ)	4	6736×6736	0.03
...mag-z9...	magnification map (μ)	9	6736×6736	0.03
...deflect-x...	deflection matrix (x, units=arcsec)	9	6736×6736	0.03
...deflect-y...	deflection matrix (y, units=arcsec)	9	6736×6736	0.03
...kappa...	convergence map (κ)	9	6736×6736	0.03
...gamma...	shear map (γ)	9	6736×6736	0.03
kappa**.fits	low rez convergence from MCMC	9	1684×1684	0.12
gamma**.fits	low rez shear from MCMC	9	1684×1684	0.12

Note. — All high-resolution FITS files are named with the same format: hlsp_frontier_model_abell2744_sharon_[column 1]_v1.fits.